

See discussions, stats, and author profiles for this publication at: <https://www.researchgate.net/publication/225305960>

# Effect of $[Fe(CN)_6]^{4-}$ Substitutions on the Spin-Flop Transition of a Layered Nickel Phyllosilicate

ARTICLE *in* LANGMUIR · JUNE 2012

Impact Factor: 4.46 · DOI: 10.1021/la3016673 · Source: PubMed

---

CITATION

1

READS

36

## 9 AUTHORS, INCLUDING:



Konstantinos Dimos

University of Ioannina

34 PUBLICATIONS 338 CITATIONS

[SEE PROFILE](#)



Ioannis Panagiotopoulos

University of Ioannina

122 PUBLICATIONS 1,482 CITATIONS

[SEE PROFILE](#)



Petra Rudolf

University of Groningen

256 PUBLICATIONS 5,688 CITATIONS

[SEE PROFILE](#)



Thomas Bakas

University of Ioannina

119 PUBLICATIONS 1,947 CITATIONS

[SEE PROFILE](#)

## Effect of $[\text{Fe}(\text{CN})_6]^{4-}$ Substitutions on the Spin-Flop Transition of a Layered Nickel Phyllosilicate

Konstantinos Dimos,\*<sup>†</sup> Ioannis Panagiotopoulos,\*<sup>†</sup> Theodoros Tsoufis,<sup>‡</sup> Régis Y. N. Gengler,<sup>‡</sup> Aliki Moukarika,<sup>§</sup> Petra Rudolf,<sup>‡</sup> Michael A. Karakassides,<sup>†</sup> Thomas Bakas,<sup>§</sup> and Dimitrios Gournis<sup>†</sup>

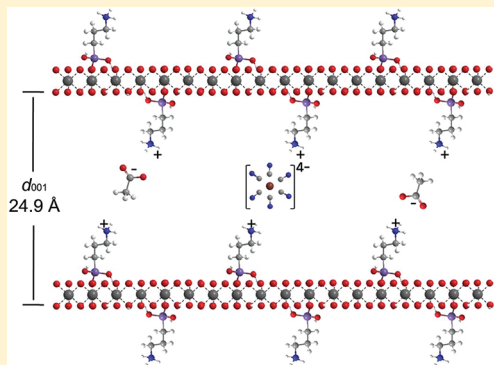
<sup>†</sup>Department of Materials Science & Engineering, University of Ioannina, GR-45110 Ioannina, Greece

<sup>‡</sup>Zernike Institute for Advanced Materials, University of Groningen, Nijenborgh 4, NL-9747 AG Groningen, The Netherlands

<sup>§</sup>Department of Physics, University of Ioannina, GR-45110 Ioannina, Greece

### S Supporting Information

**ABSTRACT:** A 3 to 1 Ni/Si antiferromagnetic layered phyllosilicate,  $\text{Ni}_3\text{Si}(\text{C}_3\text{H}_6\text{NH}_3)\text{F}_{0.65}\text{O}_{1.9}(\text{OH})_{4.45}(\text{CH}_3\text{COO})_{1.1}\cdot x\text{H}_2\text{O}$ , was modified with  $\text{K}_4[\text{Fe}(\text{CN})_6]\cdot 3\text{H}_2\text{O}$ . This compound retained its ordering as proved by X-ray diffraction, while infrared spectra revealed the presence of  $[\text{Fe}(\text{CN})_6]^{4-}$  groups and X-ray photoelectron spectroscopy showed that the latter partially substitute the acetate groups. Both the parent and the modified compound are canted antiferromagnets with an anisotropy perpendicular to the layers and show spin-flop transitions. For the parent compound, a single step spin-flop occurs at  $H = 24$  kOe. The modified compound shows increased antiferromagnetic canting and a two-step transition ( $H_1 = 24$  kOe,  $H_2 = 48$  kOe). These results testify to the existence of competing interactions that depend sensitively on the grafted species.



### INTRODUCTION

Phyllosilicates belong to the large and varied class of layered materials. These two-dimensional (2D) systems exhibit, depending on their composition, diverse properties such as ion-exchange, swelling, intercalation, high specific surface areas, shape selectivity, and exotic electronic or magnetic properties. The adaptability of their properties makes them ideal candidate materials for numerous applications as catalysts, sensors, sorbents, etc.<sup>1–3</sup> Although many naturally occurring phyllosilicates like talc have little or no ion-exchange capacity restricting their applicability, synthetic talc-like materials can exhibit ion-exchange capability together with other significant properties. Moreover, their crystallinity can be improved if hydrothermal conditions are adopted during the synthetic process.<sup>1</sup> Properties of synthetic phyllosilicates can be easily tuned because various metallic cations and trialkoxysilane precursors can be used in the copolymerization synthetic reactions.<sup>3,4</sup>

Layered nickel phyllosilicates consist of hydroxide layers of magnetic atoms separated by Si-aminopropyl groups and have recently been used as a pristine material for the development of nickel-containing magnetic nanoparticles,<sup>5–7</sup> optically active hybrids,<sup>8</sup> and effective catalytic materials.<sup>9,10</sup> Depending on the Ni/Si ratio, 1:1 or 2:1 phyllosilicates can be retrieved.<sup>3,11,12</sup> In the talc-like 2:1 phyllosilicates as in the case reported here, the inorganic layer with a thickness of ca. 9.4 Å consists of two tetrahedral silicate sheets interleaving an inner octahedral Ni(II) sheet.<sup>12</sup> These materials, if well crystallized, can be considered as model magnetic systems exhibiting several interesting and adjustable magnetic properties. As a result of

the layered nature of these materials, the magnetic interactions are anisotropic, stronger within the planes and weaker between the planes, resulting in a quasi-two-dimensional character and giving a variety of ground states depending on the ratio between interchain and intrachain interactions but due to the strong intralayer interactions the effect of the dipolar field may be also significant.<sup>13</sup> The interlayer spacing as well as the strength and sign of interlayer interactions can be adjusted chemically by inserting ions or neutral molecules into the galleries, by connecting organic groups through to the layers via covalent bonds as well as by a proper choice of the grafted silicate species and the substituted magnetic atoms. For instance, by adjusting the Ni/Si ratio, both ferromagnetic<sup>12</sup> and antiferromagnetic structures are obtained.<sup>1</sup>

$\text{Ni}_3\text{Si}(\text{C}_3\text{H}_6\text{NH}_3)\text{F}_{0.65}\text{O}_{1.9}(\text{OH})_{4.45}(\text{CH}_3\text{COO})_{1.1}\cdot x\text{H}_2\text{O}$  layered phyllosilicates have been proven<sup>1</sup> to show a layered-antiferromagnetic canted (AF) type of magnetic order below a Néel point of 21 K characterized by an easy axis perpendicular to the Ni layers. The isothermal magnetization curves show a spin-flop about 20 kOe, exhibiting a hysteresis of 2 kOe.<sup>1,14</sup>

The canted antiferromagnetism itself suggests a state that sensitively depends on the existence of competing interactions. Given the wealth of phenomena that can be obtained, this system has not yet been adequately explored. The structure consists of Ni hydroxide layers within which the exchange

Received: April 24, 2012

Revised: June 11, 2012

Published: June 13, 2012



interaction is expected to be ferromagnetic. The existence of perpendicular anisotropy implies that the antiferromagnetic coupling cannot be attributed to the dipole interactions which, in this case, would favor ferromagnetic interlayer coupling. Thus, the coupling must be mediated through the interlayer bonds. It is therefore of interest to explore the effect of substitutions on the organic part that bridges the layers and how they influence the magnetic ordering and transitions observed.

Here, we focus on the modification of the magnetic properties of a  $\text{Ni}_3\text{Si}(\text{C}_3\text{H}_6\text{N}\text{H}_3)\text{F}_{0.65}\text{O}_{1.9}-(\text{OH})_{4.45}(\text{CH}_3\text{COO})_{1.1}\cdot x\text{H}_2\text{O}$  layered phyllosilicate, prepared under hydrothermal conditions, in which the acetate groups between the layers have been replaced by the quadravalent ferrocyanide  $[\text{Fe}(\text{CN})_6]^{4-}$  groups. This substitution can be used to modify the magnetic properties and to elucidate the basic mechanisms through which magnetic order and anisotropy are defined in these materials. The obtained compounds were structurally characterized with X-ray powder diffraction measurements, FT-infrared spectroscopy, and for the first time X-ray photoelectron spectroscopy measurements. Magnetic properties were examined with SQUID and high-field magnetometry as well as Mössbauer measurements. The samples exhibited high crystallinity, canted antiferromagnetism with an anisotropy perpendicular to the layers and showed spin-flop transitions.

## EXPERIMENTAL SECTION

**Synthesis.** The organic–inorganic nickel silicates were synthesized under a hydrothermal synthetic approach at 170 °C using nickel acetate, 3-aminopropyltriethoxysilane, and ammonium fluoride as mineralizing agent. 0.6 mmol of  $\text{Ni}(\text{CH}_3\text{COO})_2\cdot 4\text{H}_2\text{O}$  was dissolved in 5 mL of  $\text{H}_2\text{O}$  in a 20 mL beaker, and 0.8 mmol of 3-aminopropyltriethoxysilane was added. In another beaker 0.2 mmol of  $\text{NH}_4\text{F}$  was dissolved in 5 mL of  $\text{H}_2\text{O}$ , and the solution was subsequently added dropwise to the first beaker. The reactants were set at 170 °C under autogenous conditions in a 75 mL autoclave and left to react for 48 h. After 2 days a light green powder was retrieved by centrifugation and rinsing with  $\text{H}_2\text{O}$ . The compound was then air-dried (this sample is denoted as parent in the following). Afterward, it was treated with  $\text{K}_4[\text{Fe}(\text{CN})_6]\cdot 3\text{H}_2\text{O}$  using a  $1\text{CH}_3\text{COO}^-/4\text{SCN}^-$  equivalent proportion under mild conditions. This acetate to cyanide equivalent proportion implies a namely 3 to 1 excess which is considered enough for ion-exchange reactions. The reactants were dissolved in 5 mL of  $\text{H}_2\text{O}$  and stirred for 4 days. Then the new compound was retrieved by centrifugation and rinsing with  $\text{H}_2\text{O}$ , and it was left to air-dry (this sample is denoted as modified in the following).

**Characterization.** The  $\theta-2\theta$  X-ray powder diffraction data (XRD) were collected with a Bruker diffractometer using  $\text{Cu K}\alpha$  radiation. Pellets of pulverized samples dispersed in  $\text{KBr}$  were used for recording FT-Infrared spectra on a Perkin-Elmer GX Fourier transform spectrometer in the frequency range of  $400-4000\text{ cm}^{-1}$ . The reported spectra are an average of 64 scans at  $2\text{ cm}^{-1}$  resolution. For the X-ray photoelectron spectroscopy (XPS) measurements, evaporated gold films supported on mica were used as substrates. The pulverized samples were dispersed in ethanol (1 wt %), and after short stirring, a small drop of the suspension was deposited on the Au substrate and left to dry in air. Samples were introduced via a load lock system into a SSX-100 (Surface Science Instruments) photoelectron spectrometer with a monochromatic  $\text{Al K}\alpha$  X-ray source ( $\hbar\nu = 1486.6\text{ eV}$ ). The base pressure in the spectrometer was  $2 \times 10^{-10}$  Torr during all measurements. The energy resolution was set to 1.16 eV to minimize measuring time. The photoelectron takeoff angle was 37°. An electron flood gun providing 0.2 eV kinetic energy electrons in combination with an Au grid placed about 1 mm above the sample was used to compensate for sample charging. All binding energies were referenced

to the C 1s core level at 285 eV. Spectral analysis included a Shirley background subtraction and peak deconvolution employing mixed Gaussian–Lorentzian functions, in a least-squares curve-fitting program (WinSpec) developed at the LISE, University of Namur, Belgium. Magnetic measurements in the field range up to 5 T were performed in a SQUID magnetometer (Quantum Design). Measurements at higher fields were carried out using a 22 T resistive magnet M6 with an extraction magnetometry setup at the Grenoble High Magnetic Field Laboratory. For the magnetic measurements, samples in the form of flakes (not pulverized) have been used. These have been prepared by settling of particles from a suspension. When this method is used, there is a preferential orientation of the *c*-axis perpendicular to the flake plane. Measurements have been performed with the applied field parallel in the flake plane and perpendicular to it by simply placing properly the flakes. Mössbauer measurements were carried out with a conventional, constant acceleration spectrometer equipped with a  $^{57}\text{Co}(\text{Rh})$  source. Spectra were obtained at room temperature and fitted with a least-squares minimization procedure assuming Lorentzian line shapes.

## RESULTS AND DISCUSSION

**Structural Characterization.** X-ray powder diffraction patterns of parent and modified compounds are shown in Figure 1. The progression of diffraction peaks at low angles can

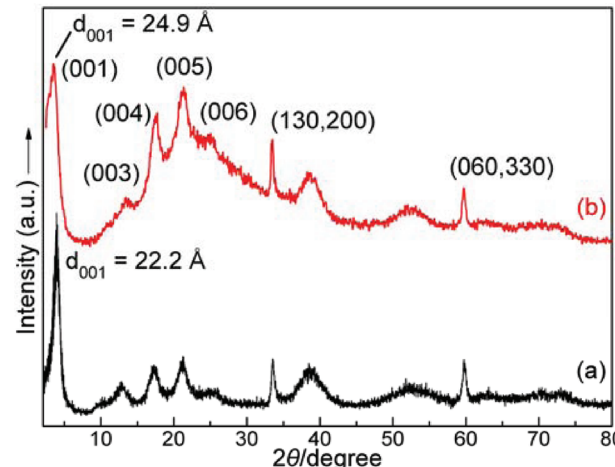


**Figure 1.** X-ray powder diffraction patterns of the parent nickel phyllosilicate (a) and a typical modified (b) sample treated with  $\text{K}_4[\text{Fe}(\text{CN})_6]\cdot 3\text{H}_2\text{O}$ .

be indexed as the (001) of the typical phyllosilicate cell, whereas the narrow peaks at  $2.679$  and  $1.550\text{ \AA}$  can be indexed as (130, 200) and (060, 330), respectively.<sup>1,11</sup> The latter are very weak in well-oriented samples in the form of flakes so pulverized samples were measured in order to enhance the in-plane diffraction peaks. Applying Bragg's law for the first reflection peak, a  $d_{001}$  spacing of  $22.2\text{ \AA}$  is calculated for the parent sample, while  $d_{001}$  spacing of the modified compound is  $24.9\text{ \AA}$ . The basal spacing of the parent sample ( $22.2\text{ \AA}$ ) is in agreement with the one reported in the literature.<sup>1</sup> As known, the 2:1 phyllosilicates have an inorganic layer consisting of two tetrahedral silicate sheets interleaving an inner octahedral metal(II) sheet with a thickness of ca.  $9.4\text{ \AA}$ .<sup>12</sup> If we assume that the propylamine groups ( $\sim 5\text{ \AA}$  in length) are perpendicular to these layers, the interlayer space is  $\sim 2.8\text{ \AA}$  and occupied by the acetate groups. In the modified sample the interlayer space is significantly increased ( $\sim 5.5\text{ \AA}$ ), confirming the insertion of the voluminous ferrocyanide groups and the substitution of the acetate groups. From the width of the peaks, the diffraction

coherence length ( $\xi$ ) can be evaluated both along the [001] direction and in the layer plane applying the Scherrer formula (Table 1). It is evident from the  $\xi$ -values along the *c*-axis that

**Table 1.**  $\xi$ -in Plane and  $\xi$ -along *c*-Axis for Parent and Modified Samples

sample	$\xi$ -in plane (Å)	$\xi$ -along the <i>c</i> -axis (Å)
parent	300–460	86
modified	280–350	50

the parent sample exhibits high crystallinity since nearly 4 layers are oriented in the powder form, while for the modified material it can be estimated that ~2 layers are stacked in a pulverized sample. The transverse coherence length is believed to define the dipolar coupling strength between the layers due to the formation of correlated spin domains.<sup>14</sup> Since no significant difference was found in the lateral coherence length ( $\xi$ -in plane) of the two samples, the differences in their magnetic behavior cannot be ascribed to differences in the dipolar coupling strength resulting from differences in structural coherence.

The FT-infrared spectrum of the parent sample in Figure 2a shows main peaks at  $\nu_{\max}$ (KBr pellets)/cm<sup>-1</sup>: 3632 s  $\nu$ (NiO-

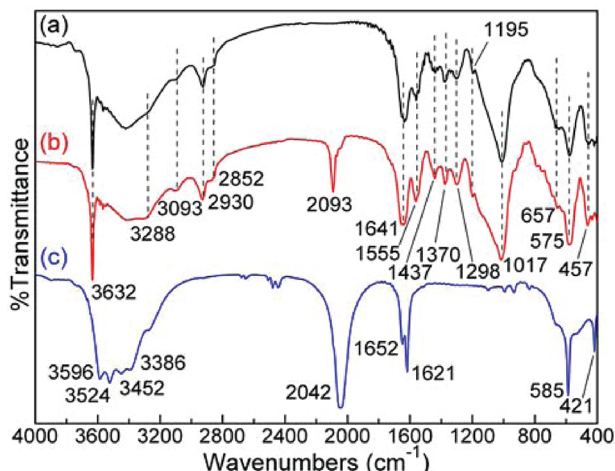


**Figure 2.** FT-infrared spectra of the parent nickel phyllosilicate (a), a typical modified compound treated with  $K_4[Fe(CN)_6] \cdot 3H_2O$  (b), and  $K_4[Fe(CN)_6] \cdot 3H_2O$  (c).

H), 3288 vw  $\nu$ (N–H), 3093 w  $\nu$ (NH<sub>3</sub><sup>+</sup>), 2930 m  $\nu_{\text{asym}}(\text{CH}_2)$ , 2852w  $\nu_{\text{sym}}(\text{CH}_2)$ , 1641 m  $\delta(\text{H}_2\text{O})$ , 1555 w  $\nu_{\text{asym}}(\text{COO}^-)$ , 1437 w  $\delta(\text{CH}_2)$ , 1370 w  $\delta(\text{CH}_2)$ , 1298 w  $\nu(\text{C}-\text{N})$ , 1195 vw  $\nu(\text{Si}-\text{C})$ , 1017 br  $\nu_{\text{asym}}(\text{Si}-\text{O}-\text{Si})$ , 657 vw  $\delta(\text{Ni}-\text{O}-\text{H})$ , 575 m  $\nu(\text{Ni}-\text{O})$ , and 457 w  $\rho(\text{Si}-\text{O}-\text{Si})$ .<sup>1,11,15,16</sup> FT-infrared spectra (a) and (b) have common peaks, while spectrum (b) of the modified sample showed an additional peak at 2093 m, which is assigned to CN<sup>-</sup> groups whose presence will be discussed later. For comparison, spectrum (c) of pure  $K_4[Fe(CN)_6] \cdot 3H_2O$  (KFCT) is also shown in Figure 2c and has main peaks at  $\nu_{\max}$ (KBr pellets)/cm<sup>-1</sup>: 3596 m  $\nu_{\text{asym}}(\text{H}_2\text{O})$ -(II) ( $\nu_3$ ), 3524 m  $\nu_{\text{asym}}(\text{H}_2\text{O})$ -(I) ( $\nu_3$ ), 3452 m  $\nu_{\text{sym}}(\text{H}_2\text{O})$ -(II) ( $\nu_1$ ), 3386 m  $\nu_{\text{sym}}(\text{H}_2\text{O})$ -(I) ( $\nu_1$ ), 2042 vs  $\nu(\text{CN})$ , 1652 m  $\delta(\text{H}_2\text{O})$ -(I), 1621 m  $\delta(\text{H}_2\text{O})$ -(II), 585 m  $\nu(\text{Fe-CN})$ , and 421 w  $\gamma(\text{H}_2\text{O})$ , where (H<sub>2</sub>O)-(I) and (H<sub>2</sub>O)-(II) denote two crystallographically different H<sub>2</sub>O molecules in the KFCT crystals.<sup>17–19</sup> The presence of the CN<sup>-</sup> peak at 2093 cm<sup>-1</sup> in

spectrum (b) of the modified sample confirms the successful insertion KFCT. Moreover, the observed shift of the original CN<sup>-</sup> peak to higher wavenumbers (ca. 50 cm<sup>-1</sup>) testifies to the formation of bridged cyano complexes such as Fe(II)–C≡N–NH<sub>3</sub>(I).<sup>20,21</sup>

The C 1s core level photoemission line of the parent compound was found to consist of three main contributions (Figure 3a). The lower binding energy component at 285 eV is

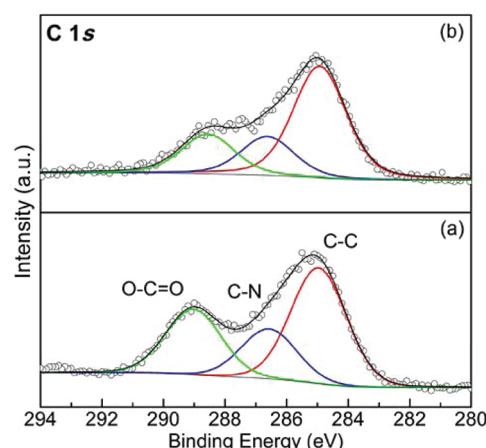


**Figure 3.** C 1s core level X-ray photoemission spectra of the parent nickel phyllosilicate (a) and a typical modified sample treated with  $K_4[Fe(CN)_6] \cdot 3H_2O$  (b).

attributed to the C–C bonds of the aliphatic chain of the aminopropylsilane that is attached to the nickel hydroxide layers. The second component, recorded at a binding energy of 286.5 eV, is assigned mainly to the C–N bonds of the amine groups which are present in the galleries between the nickel hydroxide layers. The higher binding energy component at 289 eV is due to the acetate groups (COO<sup>-</sup>) that act as counterions in the interlayer space. Similarly, the C 1s spectrum of the chemically modified nickel hydroxide (Figure 3b) testifies to the presence of C–C, C–N, and O=C=O bonds as suggested by the components at 285, 286.5, and 288.5 eV. However, the relative area ratio of (C–N)/(COO<sup>-</sup>) groups in the case of the chemically modified sample was found to be equal to 1.0, i.e., considerably higher than the corresponding value (0.75) calculated for the parent material. This suggests a decrease of the acetate groups present in the interlayer space, further confirming their partial exchange by the ferrocyanide complexes as also deduced from XRD and FT-IR results.

The successful incorporation of the ferrocyanide groups between nickel hydroxide sheets is further corroborated by the N 1s core level XPS spectra of the synthesized samples. In detail, the N 1s line of the parent material (Figure 4a) could be fitted with two contributions: a lower binding energy peak at 399.7 eV due to the amine groups (–NH<sub>2</sub>) also present in the interlayer galleries<sup>22,23</sup> and a second peak at 402.3 eV, which is attributed to protonated terminal amine groups (–NH<sub>3</sub><sup>+</sup>).<sup>24</sup> Both peaks show, within the limits of experimental error, the same binding energy values before and after partial exchange of the acetate by ferrocyanide groups (Figure 4b). An important finding in the N 1s spectrum of the modified material is the appearance of an additional peak characteristic for cyanide groups at 398 eV, which is not present in the corresponding spectrum of the parent material. This strongly suggests the successful intercalation of CN<sup>-</sup> groups within the interlayer

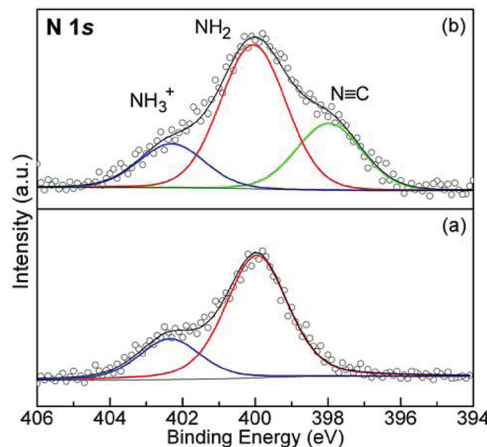


**Figure 4.** N 1s core level X-ray photoemission spectra of the parent nickel phyllosilicate (a) and a typical modified sample treated with  $K_4[Fe(CN)_6] \cdot 3H_2O$  (b).

space.<sup>25</sup> The exchange of the acetate by the ferrocyanide groups within the interlayer space is further supported by quantitative XPS results. In fact, XPS provides not only qualitative but also quantitative information,<sup>26</sup> since the peak areas normalized with the atomic sensitivity factors are proportional to the number of the corresponding atoms within the sampling depth. In this context, the relative peak area ratio C:N was found considerably higher (9.8) for the parent than for the modified sample (7.6). The decrease of the C:N ratio again confirms the removal of the acetate groups from the interlayer space and their partial replacement by the ferrocyanide groups.

No significant changes were observed in the Ni 2p<sub>3/2</sub> photoemission spectrum of the Ni phyllosilicates materials before (Figure 5a, left) and after (Figure 5b, left) the exchange

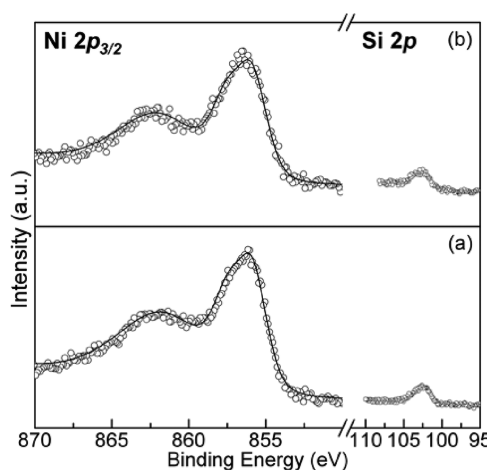


**Figure 5.** X-ray photoemission spectra of Ni 2p<sub>3/2</sub> (left) and Si 2p (right) core level regions of the parent nickel phyllosilicate (a) and a typical modified sample treated with  $K_4[Fe(CN)_6] \cdot 3H_2O$  (b).

reactions. In detail, the Ni 2p<sub>3/2</sub> core level spectra of the parent and the cyanide-modified phyllosilicates both show one peak centered at 856.6 eV followed by a broad shoulder at the higher binding energy side. 856.6 eV is a binding energy value characteristic for nickel hydroxide<sup>27,28</sup> and nickel fluoride,<sup>29</sup> both expected to be present in the inorganic framework of the nickel phyllosilicate sheets; the broad shoulder is the corresponding satellite structure.<sup>30,31</sup> For both parent and

modified phyllosilicates, the Si 2p peak (Figure 5, right) was also recorded to calculate the relative ratio of Ni:Si within sampling depth from the peak areas of nitrogen to silicon normalized with the corresponding atomic sensitivity factors. The value of the Ni:Si ratio of the parent and modified nickel phyllosilicates was found to be the same within the experimental error, indicating that the parent layered material remained unaffected upon modification with ferrocyanide anions. A schematic representation of the structure of the modified sample is shown in Figure 6 where the partial substitution of acetates by ferrocyanides is illustrated.

**Magnetic Measurements.** In the Mössbauer spectra of the modified sample (available in Supporting Information in Figure S1) only a singlet with an isomer shift of  $-0.058(1)$  mm/s appears. This indicates that the Fe atoms remain in a low-spin state and are therefore not expected to contribute to the magnetometry measurements. The observed magnetic moment is hence due exclusively to Ni atoms. Our measurements on the parent compound as well on the modified one, where the acetate groups between the layers have been replaced by the quadrivalent  $[Fe(CN)_6]^{4-}$  groups, shown in Figure 7, suggest antiferromagnetically coupled ferromagnetic layers for both compounds. More specifically, at low fields there is weak magnetic contribution that can be attributed to a “canted” antiferromagnetic (AF) structure. The latter is an AF structure in which the antiparallel alignment of the spins is imperfect, yielding a small net moment due to incomplete cancellation of the opposite spins. The curves presented in Figure 7 have been measured field cooling in an applied field of 100 Oe. Thus, the differences in magnetization values are mainly due to differences in remanence, which are related to the canting angles. The canting angles can be calculated and amount to  $1.6^\circ$  and  $3.8^\circ$  for the parent and the modified compound, respectively. The  $M$  vs  $T$  measurements (Figure 7) give an ordering temperature of 26 K for both samples. This implies that the substitution does not affect the coupling strength but mainly nonisotropic coupling terms that are responsible for the canted structure.

In the temperature range above 50 K,  $1/\chi$  shows a linear dependence on  $T$  and can be fitted to a Curie–Weiss law (Figure 8):

$$1/\chi = (T - \theta)/C \quad (1)$$

The positive intercept of the line with the temperature axis, for both samples, indicates the presence strong ferromagnetic in-plane interactions and yields Weiss constants  $\theta = 24.0 \pm 1.2$  K and  $\theta = 27.6 \pm 1.4$  K for the parent and modified samples, respectively. The effective moment, if assigned to a spin one, gives a Landé factor  $g = 2.3 \pm 0.1$  for both samples.

In the magnetization versus field curves at 5 K (Figure 9) spin-flop transitions can be observed. These transitions are observed when the magnetic field is applied along the easy anisotropy axis, which is perpendicular to the layers. The measurements with the field in-plane show that this is the hard axis and that the anisotropy field amounts to 110 kOe. To study these high field transitions, to ascertain that no further steps occur before saturation, and to estimate the anisotropy fields, measurements up to 220 kOe were performed at the Grenoble High Magnetic Field Laboratory. The results are summarized in Figure 9. The region up to 120 kOe is presented as this field was found to be sufficient to saturate the samples even in the hard direction. For the parent compound the spin-flop occurs at 24 kOe, above which the magnetization increases

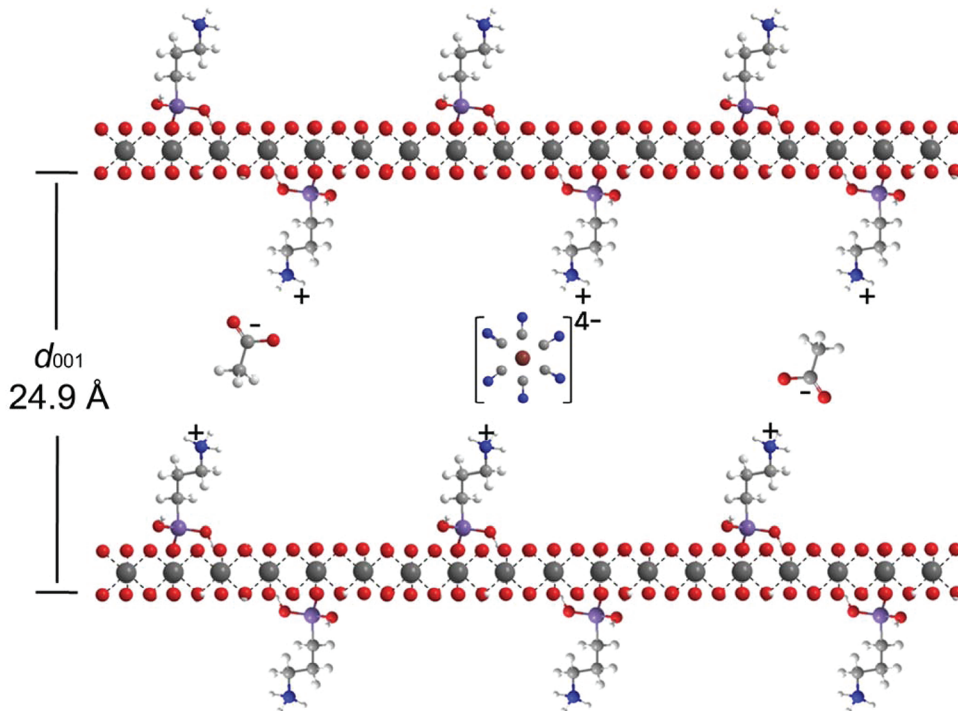


**Figure 6.** Schematic representation of the structure of the modified nickel phyllosilicate.

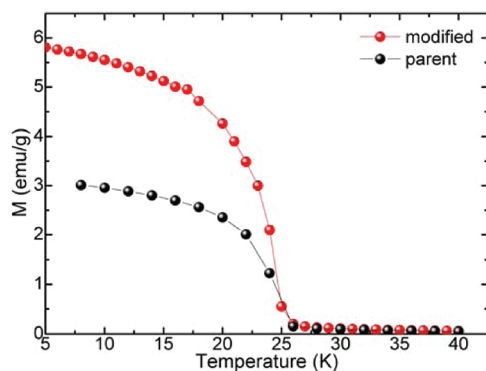


**Figure 7.** Magnetization versus temperature measurements field cooling in an applied field of 100 Oe of the parent nickel phyllosilicate and a typical modified sample treated with  $\text{K}_4[\text{Fe}(\text{CN})_6] \cdot 3\text{H}_2\text{O}$ .

continuously until saturation is reached. It can be calculated that the canting angle reaches  $7.5^\circ$  before the first spin-flop at 24 kOe occurs. For the modified compound two transitions are observed; the first one coincides with that of the parent compound but is followed by a second discontinuity observed at 48 kOe.

The field values at which the spin-flops are observed decrease, and the transitions become broader as temperature is increased. Finally above 22 K the steps are smeared out and the exact position of the spin-flops can no longer be defined. The temperature evolution of  $H_1$  and  $H_2$  is presented in the inset of Figure 9. The ratio  $H_2/H_1$  remains close to 2 at all temperatures for which both fields can be determined.

Since the XPS data show that acetate groups are partially substituted by  $[\text{Fe}(\text{CN})_6]^{4-}$ , it is tempting to assign the appearance of two steps to the simultaneous existence of two components in the modified compound. Different environments in the interlayer space could lead to different coupling strengths and spin-flop fields. Thus, the second step (at 48

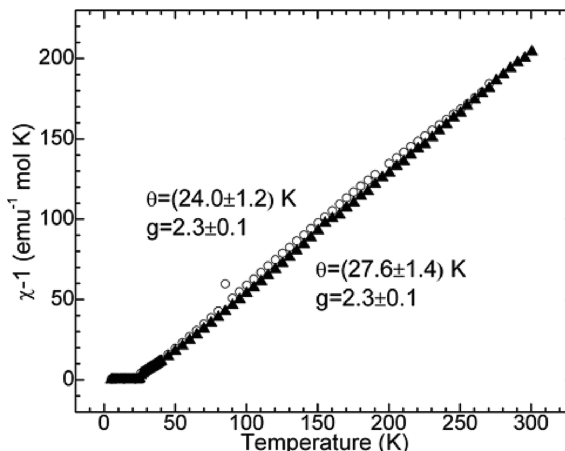


**Figure 8.** Magnetization versus temperature measured data of the parent nickel phyllosilicate (open circles) and a typical modified sample treated with  $\text{K}_4[\text{Fe}(\text{CN})_6] \cdot 3\text{H}_2\text{O}$  (closed triangles) fitted to a Curie–Weiss law.

kOe) could be attributed to the contribution from regions where  $[\text{Fe}(\text{CN})_6]^{4-}$  have substituted for acetate groups in the interlayer space. However, the existence of the strong in-plane ferromagnetic interaction ( $\theta = 27.6$  K) would average out the contribution from the randomly substituted different intercalates yielding an average response. Thus, explaining the two transitions as a result of an inhomogeneity would mean that this should occur in large spatially separated areas of the order of the in-plane structural coherence length ( $\sim 300 \text{ \AA}$ ).

On the other hand, the existence of a second transition is reminiscent of a surface spin-flop phenomenon<sup>32</sup> and due to the short structural coherence length along the film normal a strong contribution from the surfaces is expected. Two-stage spin-flop phenomena occur in finite antiferromagnetic layer systems because of inhomogeneous flopped states.<sup>32,33</sup> In our

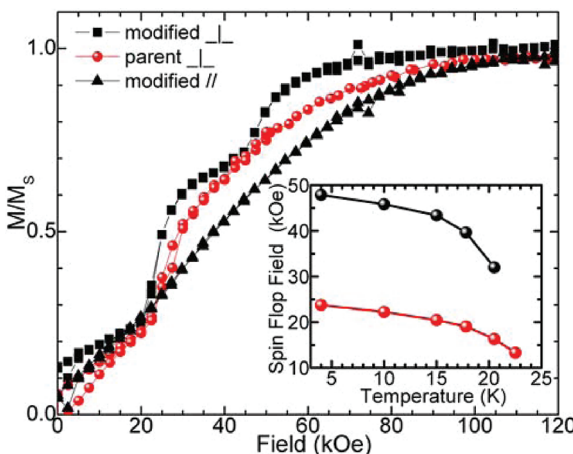


**Figure 9.** Magnetization versus field curves at 5 K for the parent nickel phyllosilicate and a typical modified sample treated with  $K_4[Fe(CN)_6] \cdot 3H_2O$ . Inset: spin-flop field versus temperature. For clarity, only the part up to 120 kOe is shown, as no further variation was observed up to 220 kOe.

case this would imply an inhomogeneous spin state along the normal to the planes that nucleates near the surface and penetrates the superlattice with increasing field.

The coexistence of competing symmetric and antisymmetric interactions of comparable magnitude is another possible mechanism that can result in two-stage spin-flop transitions.<sup>34</sup> The increased AF canting of the modified sample shows that there is indeed an increased contribution of antisymmetric interaction terms. Recently, a two-step transition was also observed in  $\beta\text{-Ni(OH)}_2$ .<sup>35,36</sup> Though the reported transitions are somewhat smeared out and become evident only when the derivative  $dM/dH$  is plotted against the magnetic field  $H$ , it is worth noticing that the values of the transition fields ( $H_1 = 28$  kOe and  $H_2 = 55$  kOe) are close those of the present study, and they also follow the relationship  $H_2/H_1 \approx 2$ . Earlier work identified only the transition at 55 kOe.<sup>37</sup> It may be concluded that these transitions occur as a result of balance of competing interaction and anisotropy terms which depend sensitively on the structural characteristics of the Ni-OH layers and their intercalated species.

## CONCLUSIONS

The magnetic properties of a 3 to 1 Ni/Si antiferromagnetic layered phyllosilicate,  $Ni_3Si(C_3H_6NH_3)F_{0.65}O_{1.9}(OH)_{4.45}(CH_3COO)_{1.1}\cdot xH_2O$ , parent compound are compared to those of a  $K_4[Fe(CN)_6] \cdot 3H_2O$  modified. XPS shows that acetates are partially substituted by  $[Fe(CN)_6]^{4-}$  groups, although the large excess of ferrocyanides used during the ion-exchange reactions. These substitutions do not influence the coupling strength between the layers and do not affect the Néel temperature; however, the AF canting angle is increased, indicating that the antisymmetric exchange terms depend sensitively on the grafted species. For the parent compound the spin-flop appears at  $H = 24$  T, while the modified compound shows increased AF canting and a two-step transition ( $H_1 = 24$  kOe,  $H_2 = 48$  kOe). This reveals that even if the substitution is not 100%, a second spin-flop transition is present in the modified sample at double the field of the first, which is also observed in another totally different magnetic system of  $\text{Ni(OH)}_2$ .

## ASSOCIATED CONTENT

### S Supporting Information

Mössbauer spectra of modified sample in Figure S1. This material is available free of charge via the Internet at <http://pubs.acs.org>.

## AUTHOR INFORMATION

### Corresponding Author

\*E-mail: kdimos@cc.uoi.gr (K.D.); ipanagio@cc.uoi.gr (I.P.).

### Notes

The authors declare no competing financial interest.

## ACKNOWLEDGMENTS

The authors acknowledge the use of magnet M6 at the Grenoble High Magnetic Field Laboratory. This work received support from the “Top Research School” program of the Zernike Institute for Advanced Materials under the Bonus Incentive Scheme (BIS) of The Netherlands’ Ministry of Education, Science, and Culture.

## REFERENCES

- (1) Richard-Plouet, M.; Vilminot, S.; Guillot, M.; Kurmoo, M. Canted Antiferromagnetism in an Organo-modified Layered Nickel Phyllosilicate. *Chem. Mater.* **2002**, *14*, 3829–3836.
- (2) Taibi, M.; Ammar, S.; Jouini, N.; Fiévet, F.; Molinié, P.; Drillon, M. Layered nickel hydroxide salts: synthesis, characterization and magnetic behaviour in relation to the basal spacing. *J. Mater. Chem.* **2002**, *12*, 3238–3244.
- (3) da Fonseca, M. G.; Silva, C. R.; Barone, J. S.; Airoldi, C. Layered hybrid nickel phyllosilicates and reactivity of the gallery space. *J. Mater. Chem.* **2000**, *10*, 789–795.
- (4) Richard-Plouet, M.; Vilminot, S. Ferromagnetism in talk-like cobalt-phyllosilicates. *Solid State Sci.* **1999**, *1*, 381–393.
- (5) McDonald, A.; Scott, B.; Villemure, G. Hydrothermal preparation of nanotubular particles of a 1:1 nickel phyllosilicate. *Microporous Mesoporous Mater.* **2009**, *120*, 263–266.
- (6) Richard-Plouet, M.; Guillot, M.; Vilminot, S.; Leuvrey, C.; Estournès, C.; Kurmoo, M. *hcp* and *fcc* Nickel Nanoparticles Prepared from Organically Functionalized Layered Phyllosilicates of Nickel(II). *Chem. Mater.* **2007**, *19*, 865–871.
- (7) Park, J. C.; Lee, H. J.; Bang, J. U.; Park, K. H.; Song, H. Chemical transformation and morphology change of nickel–silica hybrid nanostructures via nickel phyllosilicates. *Chem. Commun.* **2009**, 7345–7347.
- (8) Richard-Plouet, M.; Vilminot, S.; Guillot, M. Synthetic transition metal phyllosilicates and organic-inorganic related phases. *New J. Chem.* **2004**, *28*, 1073–1082.
- (9) Sivaiah, M. V.; Petit, S.; Beaufort, M. F.; Eyidi, D.; Barrault, J.; Batiot-Dupeyrat, C.; Valange, S. Nickel based catalysts derived from hydrothermally synthesized 1:1 and 2:1 phyllosilicates as precursors for carbon dioxide reforming of methane. *Microporous Mesoporous Mater.* **2011**, *140*, 69–80.
- (10) Sivaiah, M. V.; Petit, S.; Barrault, J.; Batiot-Dupeyrat, C.; Valange, S. CO<sub>2</sub> reforming of CH<sub>4</sub> over Ni-containing phyllosilicates as catalyst precursors. *Catal. Today* **2010**, *157*, 397–403.
- (11) Guillot, M.; Richard-Plouet, M.; Vilminot, S. Structural characterisations of a lamellar organic–inorganic nickel silicate obtained by hydrothermal synthesis from nickel acetate and (aminopropyl)triethoxysilane. *J. Mater. Chem.* **2002**, *12*, 851–857.
- (12) Richard-Plouet, M.; Vilminot, S. Magnetic properties of two-dimensional triangular arrays of Ni ions in nickel phyllosilicates. *J. Mater. Chem.* **1998**, *8*, 131–137.
- (13) Lee, K. W.; Lee, C. E. Ground-state crossover in the quasi-two-dimensional classical Heisenberg model with dipolar-type interaction. *Phys. Rev. B* **2003**, *68*, 134437(1–5).

- (14) Drillon, M.; Panissod, P.; Souletie, P. R. J.; Ksenofontov, V.; Gütlich, P. Pressure effect on the magnetism of layered copper(II) compounds with interlayer spacing up to 40.7 Å: Nature of the magnetic ordering. *Phys. Rev. B* **2002**, *65*, 104404(1–8).
- (15) Dimos, K.; Jankovič, L.; Koutselas, I. B.; Karakassides, M. A.; Zbořil, R.; Komadel, P. Low-Temperature Synthesis and Characterization of Gallium Nitride Quantum Dots in Ordered Mesoporous Silica. *J. Phys. Chem. C* **2012**, *116*, 1185–1194.
- (16) Hengbin, Z.; Hansan, L.; Xuejing, C.; Shujia, L.; Chiachung, S. Preparation and properties of the aluminum-substituted  $\alpha$ -Ni(OH)<sub>2</sub>. *Mater. Chem. Phys.* **2003**, *79*, 37–42.
- (17) Gaffar, M. A.; Abd-Elrahman, M. I. Vibration Spectra of Ferrocyanide Ions in the Paraelectric Phase of K<sub>4</sub>[Fe(CN)<sub>6</sub>] · 3H<sub>2</sub>O. *Phys. Status Solidi B* **2001**, *225*, 271–287.
- (18) Gaffar, M. A.; Abd-Elrahman, M. I. Vibration spectra of water molecules in the paraelectric phase of K<sub>4</sub>[Fe(CN)<sub>6</sub>] · 3H<sub>2</sub>O. *Physica B* **2001**, *304*, 423–436.
- (19) Kanagadurai, R.; Sankar, R.; Sivanesan, G.; Srinivasan, S.; Jayavel, R. Growth and properties of ferroelectric potassium ferrocyanide trihydrate single crystals. *Cryst. Res. Technol.* **2006**, *41*, 853–858.
- (20) Nakamoto, K. *Infrared and Raman Spectra of Inorganic and Coordination Compounds*, 4th ed.; J. Wiley & Sons Inc.: New York, 1986; pp 278–279.
- (21) Shriver, D. F.; Posner, J. Bridge Addition Compounds. III. The Influence of Boron-Containing Lewis Acids on Electronic Spectra, Vibrational Spectra, and Oxidation Potentials of Some Iron-Cyanide Complexes. *J. Am. Chem. Soc.* **1966**, *88*, 1672–1677.
- (22) Pavlidis, I. V.; Vorhaben, T.; Tsoufis, T.; Rudolf, P.; Bornscheuer, U.; Gournis, D.; Stamatis, H. Development of effective nanobiocatalytic systems through the immobilization of hydrolases on functionalized carbon-based nanomaterials. *Bioresour. Technol.* **2012**, *115*, 164–171.
- (23) Tzialla, A. A.; Pavlidis, I. V.; Felicissimo, M. P.; Rudolf, P.; Gournis, D.; Stamatis, H. Lipase immobilization on smectite nanoclays: Characterization and application to the epoxidation of  $\alpha$ -pinene. *Bioresour. Technol.* **2010**, *101*, 1587–1594.
- (24) Gournis, D.; Jankovic, L.; Maccallini, E.; Benne, D.; Rudolf, P.; Colomer, J.-F.; Sooambar, C.; Georgakilas, V.; Prato, M.; Fanti, M.; Zerbetto, F.; Sarova, G. H.; Guldi, D. M. Clay–Fulleropyrrolidine Nanocomposites. *J. Am. Chem. Soc.* **2006**, *128*, 6154–6163.
- (25) Gournis, D.; Papachristodoulou, C.; Maccallini, E.; Rudolf, P.; Karakassides, M. A.; Karamanis, D. T.; Sage, M. H.; Palstra, T. T. M.; Colomer, J. F.; Papavasileiou, K. D.; Melissas, V. S.; Gangas, N. H. A two-dimensional magnetic hybrid material based on intercalation of a cationic Prussian blue analog in montmorillonite nanoclay. *J. Colloid Interface Sci.* **2010**, *348*, 393–401.
- (26) Briggs, D.; Seah, M. P. *Practical Surface Analysis*; John Wiley: Chichester, 1990.
- (27) Lorenz, P.; Finster, J.; Wendt, G.; Salyn, J. V.; Zumadilov, E. K.; Nefedov, V. I. Esca investigations of some NiO/SiO<sub>2</sub> and NiO–Al<sub>2</sub>O<sub>3</sub>/SiO<sub>2</sub> catalysts. *J. Electron Spectrosc. Relat. Phenom.* **1979**, *16*, 267–276.
- (28) McIntyre, N. S.; Cook, M. G. X-ray photoelectron studies on some oxides and hydroxides of cobalt, nickel, and copper. *Anal. Chem.* **1975**, *47*, 2208–2213.
- (29) Löchel, B. P.; Strehblow, H. H. Breakdown of Passivity of Nickel by Fluoride. *J. Electrochem. Soc.* **1984**, *131*, 713–723.
- (30) Moreno-Castilla, C.; Maldonado-Hódar, F. J.; Pérez-Cadenas, A. F. Physicochemical Surface Properties of Fe, Co, Ni, and Cu-Doped Monolithic Organic Aerogels. *Langmuir* **2003**, *19*, 5650–5655.
- (31) Li, H.; Li, H.; Dai, W.-L.; Wang, W.; Fang, Z.; Deng, J.-F. XPS studies on surface electronic characteristics of Ni–B and Ni–P amorphous alloy and its correlation to their catalytic properties. *Appl. Surf. Sci.* **1999**, *152*, 25–34.
- (32) te Velthuis, S. G. E.; Jiang, J. S.; Bader, S. D.; Felcher, G. P. Spin Flop Transition in a Finite Antiferromagnetic Superlattice: Evolution of the Magnetic Structure. *Phys. Rev. Lett.* **2002**, *89*, 127203(1–4).
- (33) Rößler, U. K.; Bogdanov, A. N. Finite-size effects and “surface spin-flop” phenomena in antiferromagnetically coupled multilayers. *J. Alloys Compd.* **2006**, *423*, 153–158.
- (34) Tsukada, I.; Takeya, J.; Masuda, T.; Uchinokura, K. Two-Stage Spin-Flop Transitions in the  $S = 1/2$  Antiferromagnetic Spin Chain BaCu<sub>2</sub>Si<sub>2</sub>O<sub>7</sub>. *Phys. Rev. Lett.* **2001**, *87*, 127203(1–4).
- (35) Rall, J. D.; Seehra, M. S.; Shah, N.; Huffman, G. P. Comparison of the nature of magnetism in  $\alpha$ -Ni(OH)<sub>2</sub> and  $\beta$ -Ni(OH)<sub>2</sub>. *J. Appl. Phys.* **2010**, *107*, 09B511–09B511–3.
- (36) Rall, J. D.; Seehra, M. S. The nature of the magnetism in quasi-2D layered  $\alpha$ -Ni(OH)<sub>2</sub>. *J. Phys.: Condens. Matter* **2012**, *24*, 076002(1–8).
- (37) Takada, T.; Bando, Y.; Kiyama, M.; Miyamoto, H.; Sato, T. The Magnetic Property of Ni(OH)<sub>2</sub>. *J. Phys. Soc. Jpn.* **1966**, *21*, 2745–2746.